

# **$\pi$ -Stacking Synthons Repetitiveness in Coordination Compounds**

**Hamid Reza Khavasi,\* Sima Kavand**

*Faculty of Chemistry, Shahid Beheshti University, G. C., Evin, Tehran 1983963113, Iran*

## Experimental Section

**Chemicals and instrumentation.** All chemicals were purchased from Aldrich or Merck and used without further purification. The synthesis and recrystallization of *N*-(1-chloronaphthalen-4-yl)pyrazine-2-carboxamide and *N*-(1-bromonaphthalen-4-yl)pyrazine-2-carboxamide ligands and compounds **1-6** were carried out in air. Infrared spectra (4000–250 cm<sup>-1</sup>) of solid samples were taken as 1% dispersions in KBr pellets using a BOMEM-MB102 spectrometer. Elemental analysis was performed using a Heraeus CHN-O Rapid analyzer. Melting point was obtained by a Bamstead Electrothermal type 9200 melting point apparatus and corrected.

**Single crystal diffraction studies.** X-ray data for compounds  $L^{4Cl-1-naph}_{pyz-amid}$  and  $L^{4Br-1-naph}_{pyz-amid}$  and complexes  $[Hg_2Cl_4(L^{4Cl-1-naph}_{pyz-amid})_2]$ , **1**,  $[Hg_2Br_4(L^{4Cl-1-naph}_{pyz-amid})_2]$ , **2**,  $[HgI_2(L^{4Cl-1-naph}_{pyz-amid})]$ , **3**,  $[Hg_2Cl_4(L^{4Br-1-naph}_{pyz-amid})_2]$ , **4**,  $[HgBr_2(L^{4Br-1-naph}_{pyz-amid})_2]$ , **5**, and  $[HgI_2(L^{4Br-1-naph}_{pyz-amid})]$ , **6**, were collected on a STOE IPDS-II diffractometer with graphite monochromated Mo-K $\alpha$  radiation. For  $L^{4Cl-1-naph}_{pyz-amid}$  a colorless block crystal, for  $L^{4Br-1-naph}_{pyz-amid}$ ,  $[Hg_2Cl_4(L^{4Cl-1-naph}_{pyz-amid})_2]$ , **1**,  $[Hg_2Br_4(L^{4Cl-1-naph}_{pyz-amid})_2]$ , **2** and  $[HgI_2(L^{4Cl-1-naph}_{pyz-amid})]$ , **3**, a yellow block crystal, for  $[Hg_2Cl_4(L^{4Br-1-naph}_{pyz-amid})_2]$ , **4**, a light violet prism crystal and for  $[HgBr_2(L^{4Br-1-naph}_{pyz-amid})_2]$ , **5**, and  $[HgI_2(L^{4Br-1-naph}_{pyz-amid})]$ , **6**, a colorless needle crystal was chosen using a polarizing microscope and they were mounted on a glass fiber which was used for data collection. Cell constants and an orientation matrix for data collection were obtained by least-squares refinement of diffraction data from 3416 for  $L^{4Cl-1-naph}_{pyz-amid}$ , 4477 for  $L^{4Br-1-naph}_{pyz-amid}$ , **4306** for **1**, 3293 for **2**, 3786 for **3**, 5550 for **4**, 1568 for **5** and 2066 for **6** unique reflections. Data were collected at a temperature of 298(2) K to a maximum  $\theta$  value of 29.19° for  $L^{4Cl-1-naph}_{pyz-amid}$ , 32.23° for  $L^{4Br-1-naph}_{pyz-amid}$ , 29.15° for **1**, 29.20° for **2**, 29.23° for **3**, 31.96° for **4**, 29.25° for **5** and 29.45° for **6** and in a series of  $\omega$  scans in 1° oscillations and integrated using the Stoe X-Area<sup>S1</sup> software package. A numerical absorption correction was applied using the X-RED<sup>S2</sup> and X-SHAPE<sup>S3</sup> software's. The data were corrected for Lorentz and Polarizing effects. The structures were solved by direct methods<sup>S4</sup> and subsequent different Fourier maps and then refined on  $F^2$  by a full-matrix least-square procedure<sup>S4</sup> using anisotropic displacement parameters. All hydrogen atoms were added at ideal positions and constrained to ride on their parent atoms, with  $U_{iso}(H) = 1.2U_{eq}$ . All refinements were performed using the X-STEP32 crystallographic software package.<sup>S5</sup> Structural illustrations have been

drawn with ORTEP-3<sup>S6</sup> and MERCURY.<sup>S7</sup> Crystallographic data for compounds  $L^{4Cl-1-naph}_{pyz-amid}$  and  $L^{4Br-1-naph}_{pyz-amid}$  and complexes **1-6** are listed in Table 1. Selected bond distances and angles are summarized in Table 2.

**Synthesis of  $N$ -(1-chloronaphthalen-4-yl)pyrazine-2-carboxamide,  $L^{4Cl-1-naph}_{pyz-amid}$ , and  $N$ -(1-bromonaphthalen-4-yl)pyrazine-2-carboxamide,  $L^{4Br-1-naph}_{pyz-amid}$ , ligands.** A solution of 5 mmol of 1-amino-4-halonaphthalen in 5 mL pyridine was added to a solution of 5 mmol of pyrazine-2-carboxylic acid (0.62 g) in 10 mL pyridine. The resulting solution was stirred at 40°C for 30 min, then 5 mmol of triphenylphosphite (1.3 mL) was added dropwise, and the reaction mixture was stirred at 80°C for 5 h and at room temperature for 24 h. The solvent of resulting oily solution was evaporated, then the greasy product was washed with acetone, filtered and then washed with 50 mL cold methanol. A yellow powder resulted with a yield of 50%, Mp 198-202°C for  $L^{4Cl-1-naph}_{pyz-amid}$  and yellow powder resulted with a yield of 45% and Mp 201- 208°C for  $L^{4Br-1-naph}_{pyz-amid}$ . Anal. Calcd for  $L^{4Cl-1-naph}_{pyz-amid}$  (C<sub>15</sub>H<sub>10</sub>ClN<sub>3</sub>O): C, 63.50; H, 3.55; N, 14.81. Found: C, 63.55; H, 3.59; N, 14.87. FT-IR (KBr pellet, cm<sup>-1</sup>): 3358m, 1689s, 1543s, 1385m, 1096m, 824s. Anal. Calcd for  $L^{4Br-1-naph}_{pyz-amid}$  (C<sub>15</sub>H<sub>10</sub>BrN<sub>3</sub>O): C, 54.90; H, 3.07; N, 12.81. Found: C, 54.93; H, 3.12; N, 12.85. FT-IR (KBr pellet, cm<sup>-1</sup>): 3360m, 1689s, 1541s, 1385m, 1013m, 824s.

**Synthesis of Mercury(II) complexes;** [Hg<sub>2</sub>Cl<sub>4</sub>( $L^{4Cl-1-naph}_{pyz-amid}$ )<sub>2</sub>], **1**, [Hg<sub>2</sub>Br<sub>4</sub>( $L^{4Cl-1-naph}_{pyz-amid}$ )<sub>2</sub>], **2**, [HgI<sub>2</sub>( $L^{4Cl-1-naph}_{pyz-amid}$ )], **3**, [Hg<sub>2</sub>Cl<sub>4</sub>( $L^{4Br-1-naph}_{pyz-amid}$ )<sub>2</sub>], **4**, [HgBr<sub>2</sub>( $L^{4Br-1-naph}_{pyz-amid}$ )<sub>2</sub>], **5**, and [HgI<sub>2</sub>( $L^{4Br-1-naph}_{pyz-amid}$ )], **6**. To a solution of 0.5 mmol of mercury(II) halide (HgX<sub>2</sub>, X = Br and I) in 5 mL of methanol, a solution of 0.5 mmol of ligand in 5 mL methanol was added with stirring. The mixture was heated at 60°C for about 30 min and then filtered. Upon slow evaporation of the filtrate at room temperature, yellow block crystals for **1**, **2** and **3**, light violet prism crystal for **4** and colorless needled crystals for **5** and **6**, suitable for X-ray analysis, were obtained after *ca.* two weeks (yield: 70%, 65%, 55%, 50%, 52% and 60% for 1-6, respectively).

**1.** Mp: 220-223°C. Anal. Calcd for C<sub>15</sub>H<sub>10</sub>Cl<sub>3</sub>HgN<sub>3</sub>O: C, 32.44; H, 1.81; N, 7.57. Found: C, 32.48; H, 1.85; N, 7.60. FT-IR (KBr pellet, cm<sup>-1</sup>): 3360m, 1687s, 1541s, 1390m, 1111m, 830m.

**2.** Mp: 239-241°C. Anal. Calcd for C<sub>15</sub>H<sub>10</sub>Br<sub>2</sub>ClHgN<sub>3</sub>O: C, 27.97; H, 1.56; N, 6.52. Found: C, 28.01; H, 1.60; N, 6.55. FT-IR (KBr pellet, cm<sup>-1</sup>): 3353m, 1689s, 1543s, 1388m, 1112m, 828m.

3. Mp: 206-209°C. Anal. Calc. for C<sub>15</sub>H<sub>10</sub>ClHgI<sub>2</sub>N<sub>3</sub>O: C, 24.41; H, 1.37; N, 5.69. Found: C, 24.43; H, 1.40; N, 5.72. FT-IR (KBr pellet, cm<sup>-1</sup>): 3360m, 1690s, 1542s, 1389m, 1110m, 829m.
4. Mp: 240-244°C. Anal. Calcd for C<sub>15</sub>H<sub>10</sub>BrCl<sub>2</sub>HgN<sub>3</sub>O: C, 30.04; H, 1.68; N, 7.00. Found: C, 30.08; H, 1.73; N, 7.03. FT-IR (KBr pellet, cm<sup>-1</sup>): 3340m, 1692s, 1541s, 1385m, 1109m, 825m.
5. Mp (decomposed): 252-254°C. Anal. Calc. for C<sub>15</sub>H<sub>10</sub>Br<sub>3</sub>HgN<sub>3</sub>O: C, 26.17; H, 1.46; N, 6.10. Found: C, 26.21; H, 1.50; N, 6.13. FT-IR (KBr pellet, cm<sup>-1</sup>): 3333m, 1689s, 1545s, 1352m, 1026m, 832m.
6. Mp: 213-219°C. Anal. Calc. for C<sub>15</sub>H<sub>10</sub>BrHgI<sub>2</sub>N<sub>3</sub>O: C, 23.03; H, 1.29; N, 5.37. Found: C, 23.07; H, 1.32; N, 5.40. FT-IR (KBr pellet, cm<sup>-1</sup>): 3344m, 1691s, 1542s, 1380m, 1025m, 8321m.

**Computational Details.** DFT calculations were performed using the ORCA quantum chemistry suite.<sup>S8</sup> The local density approximation (LDA) exchange correlation potential was used with the local density approximation of the correlation energy.<sup>S9</sup> Gradient-corrected geometry optimizations<sup>S10</sup> were performed by using the generalized gradient approximation.<sup>S11</sup> Large atom basis sets TZP are used to ascribe all the atoms here. Scalar relativistic effects were taken into account by using the zeroth-order regular approximation (ZORA).<sup>S12</sup>

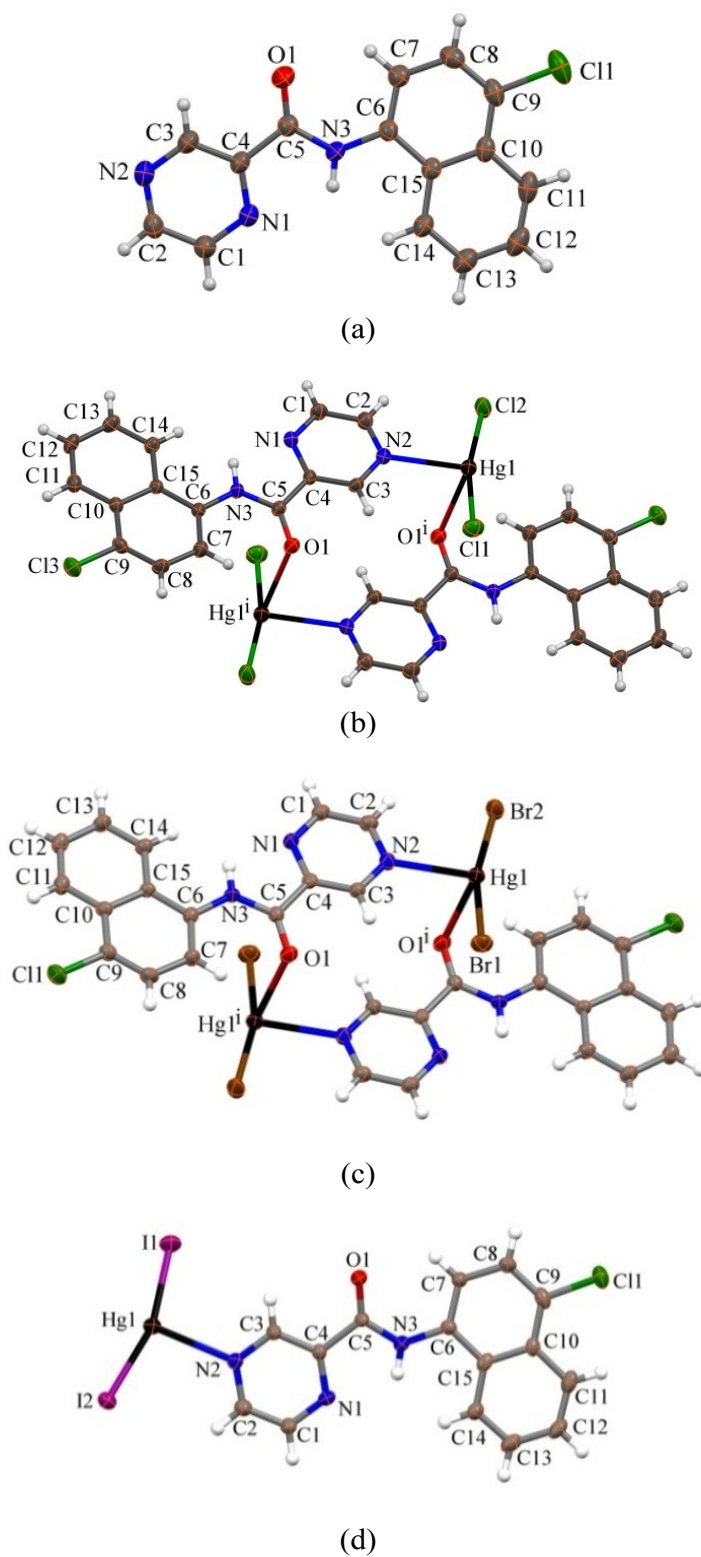


**Figure S1.** ORTEP diagram of  $L^{4Cl-1-naph}$   $pyz-amid$ , (a) and coordination compounds formed between this ligand and  $HgCl_2$ , **1**, (b),  $HgBr_2$ , **2**, (c), and  $HgI_2$ , **3**, (d), showing coordination geometry around central metal. Ellipsoids are drawn at 30% probability level. Symmetry codes: i) 1-x, 1-y, 1-z.

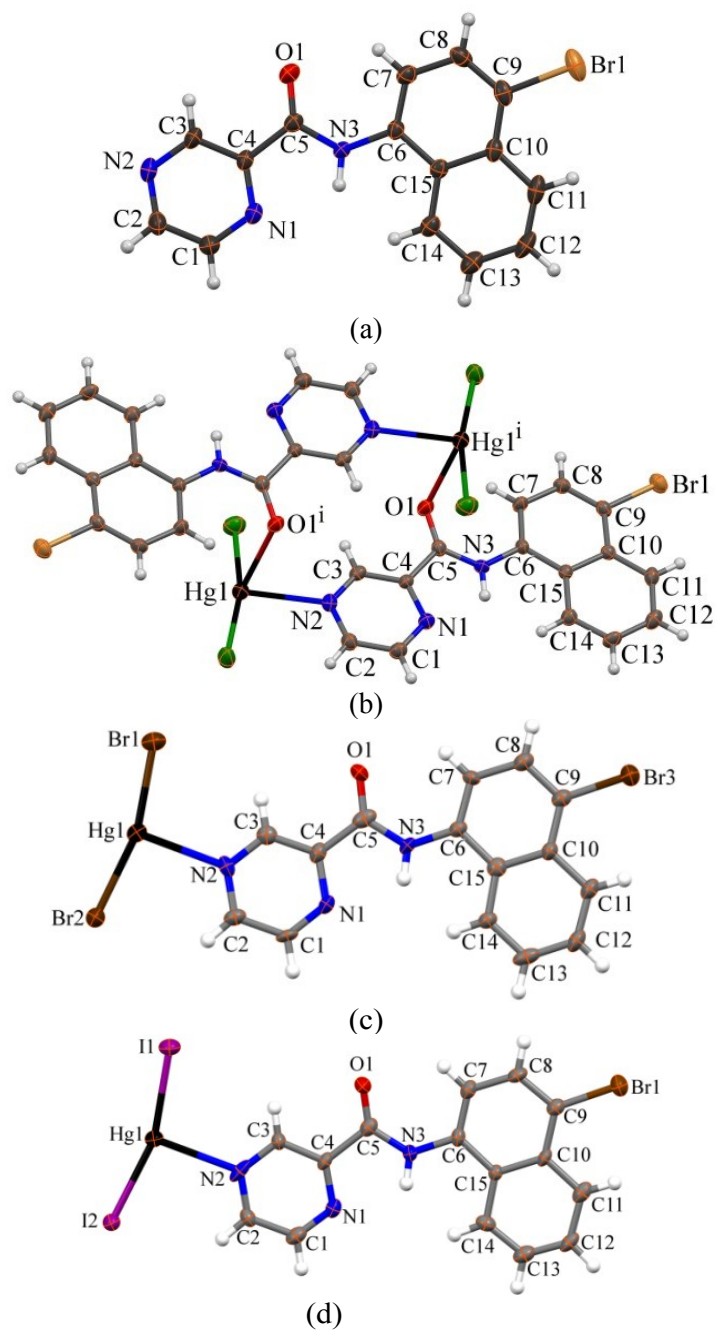


**Figure S2.** ORTEP diagram of  $L^{4Br-1-naph-pyz-amid}$ , (a) and coordination compounds formed between this ligand and  $HgCl_2$ , **4**, (b),  $HgBr_2$ , **5**, (c), and  $HgI_2$ , **6**, (d), showing coordination geometry around central metal. Ellipsoids are drawn at 30% probability level. Symmetry codes: i) 1-x, 1-y, 1-z.

**Table S1.** Structural data and refinement for  $L^{4Cl-1-naph}_{pyz-amid}$ ,  $L^{4Cl-1-naph}_{pyz-amid}$  and complexes **1-6**.

	$L^{4Cl-1-naph}_{pyz-amid}$	$L^{4Br-1-naph}_{pyz-amid}$	Complex 1	Complex 2	Complex 3	Complex 4	Complex 5	Complex 6
formula	C <sub>15</sub> H <sub>10</sub> Cl N <sub>3</sub> O	C <sub>15</sub> H <sub>10</sub> Br N <sub>3</sub> O	C <sub>15</sub> H <sub>10</sub> Cl <sub>3</sub> HgN <sub>3</sub> O	C <sub>15</sub> H <sub>10</sub> Br <sub>2</sub> Cl HgN <sub>3</sub> O	C <sub>15</sub> H <sub>10</sub> Cl HgI <sub>2</sub> N <sub>3</sub> O	C <sub>15</sub> H <sub>10</sub> BrCl <sub>2</sub> HgI <sub>2</sub> N <sub>3</sub> O	C <sub>15</sub> H <sub>10</sub> Br <sub>3</sub> HgN <sub>3</sub> O	C <sub>15</sub> H <sub>10</sub> Cl HgI <sub>2</sub> N <sub>3</sub> O
fw	283.71	283.71	555.20	644.10	738.10	599.65	688.55	782.44
$\lambda/\text{\AA}$	0.71073	0.71073	0.71073	0.71073	0.71073	0.71073	0.71073	0.71073
$T/K$	298(2)	298(2)	298(2)	298(2)	298(2)	298(2)	298(2)	298(2)
crystal.system	Monoclinic	Monoclinic	Triclinic	Triclinic	Triclinic	Triclinic	Monoclinic	Monoclinic
space group	$P2_1/n$	$P2_1/n$	$P\bar{1}$	$P\bar{1}$	$P\bar{1}$	$P\bar{1}$	$P2_1/m$	$P2_1/m$
$a/\text{\AA}$	5.0499(7)	5.1029(7)	7.7489(11)	7.8587(9)	8.5716(7)	7.8032(7)	9.8327(14)	10.133(3)
$b/\text{\AA}$	13.8171(11)	13.9355(14)	9.6446(12)	9.8104(10)	9.8507(9)	9.6586(9)	6.6591(13)	6.7797(17)
$c/\text{\AA}$	18.221(2)	18.293(3)	11.3533(13)	11.5257(13)	11.6901(10)	11.4038(11)	12.8974(17)	13.077(3)
$\omega^\circ$	90	90	77.812(9)	76.986(8)	103.615(7)	78.367(7)	90	90
$\beta^\circ$	93.432(10)	92.318(10)	81.537(10)	80.953(9)	103.475(7)	81.780(7)	91.698(11)	91.44(2)
$\gamma^\circ$	90	90	76.841(10)	75.314(9)	102.305(7)	76.496(7)	90	90
$V/\text{\AA}^3$	1269.1(3)	1299.71(3)	803.20(18)	832.75(16)	894.64(13)	814.39(13)	844.1(2)	898.1(4)
$D_{\text{calc}}/\text{Mg m}^{-3}$	1.485	1.677	2.296	2.569	2.740	2.445	2.709	2.894
$Z$	4	4	2	2	2	2	2	2
$\mu/\text{mm}^{-1}$	0.299	3.160	10.086	14.205	12.208	12.236	16.223	14.237
$F(000)$	584	656	520	592	664	556	628	700
$2\theta^\circ$	58.38	64.46	58.30	58.40	58.46	63.92	58.90	58.90
$R(\text{int})$	0.1001	0.1001	0.0825	0.0645	0.1147	0.0475	0.1100	0.1140
GOOF	1.201	1.194	1.085	1.049	1.044	1.191	1.149	1.099
$R_1^a(I > 2\sigma(I))$	0.0989	0.0850	0.0481	0.0479	0.0763	0.0410	0.0906	0.0719
$wR_2^b(I > 2\sigma(I))$	0.1368	0.1569	0.1119	0.0975	0.1888	0.1047	0.1710	0.1856
CCDC No.	1016903	1016902	1016906	1016905	1016904	1016901	1016900	1016899

$$^a R_1 = \frac{\sum ||F_o| - |F_c||}{\sum |F_o|}, \quad ^b wR_2 = \left[ \frac{\sum (w(F_o^2 - F_c^2)^2)}{\sum w(F_o^2)^2} \right]^{1/2}.$$

**Table S2.** Selected bond length (Å) and angles (°) around mercury(II) for complexes **1-6**. Symmetry codes: (i) 1-x, 1-y, 1-z.

		Complex		
		<b>1 (X = Cl)</b>	<b>2 (X = Br)</b>	<b>3 (X = I)</b>
Bond distance	Hg1-X1	2.298(2)	2.422(1)	2.596(1)
	Hg1-X2	2.309(2)	2.425(1)	2.598(1)
	Hg1-N2	2.532(6)	2.528(6)	2.544(8)
	Hg1-O1 <sup>i</sup>	2.905(6)	2.944(6)	-
Bond angle	X1-Hg1-X2	165.92(8)	163.59(3)	161.91(4)
	X1-Hg1-N2	100.0(1)	100.72(13)	98.1(2)
	X2-Hg1-N2	93.9(1)	95.52(13)	99.0(1)
	X1-Hg1-O1 <sup>i</sup>	84.6(1)	87.4(1)	-
	X2-Hg1-O1 <sup>i</sup>	100.9(1)	98.4(1)	-
	N2-Hg1-O1 <sup>i</sup>	77.4(2)	77.8(2)	-
		<b>4 (X = Cl)</b>	<b>5 (X = Br)</b>	<b>6 (X = I)</b>
Bond distance	Hg1-X1	2.299(2)	2.413(3)	2.576(2)
	Hg1-X2	2.297(2)	2.450(3)	2.604(2)
	Hg1-N2	2.522(6)	2.494(2)	2.537(2)
	Hg1-O1 <sup>i</sup>	2.942(5)	-	-
Bond angle	X1-Hg1-X2	165.81(8)	164.36(1)	162.63(6)
	X1-Hg1-N2	94.8(1)	100.1(4)	100.7(5)
	X2-Hg1-N2	99.2(1)	95.56(4)	96.7(5)
	X1-Hg1-O1 <sup>i</sup>	100.8(1)	-	-
	X2-Hg1-O1 <sup>i</sup>	85.0(1)	-	-
	N2-Hg1-O1 <sup>i</sup>	76.3(2)	-	-

## REFERENCES:

S1. *X-AREA: Program for the Acquisition and Analysis of Data*, vesion 1.30; Stoe & Cie GmbH: Darmstadt, Germany, 2005.

S2. *X-RED: Program for Data Reduction and Absorption Correction*, vesion 1.28b; Stoe & Cie GmbH: Darmstadt, Germany, 2005.

S3. *X-SHAPE: Program for crystal optimization for numerical absorption correction*, vesion 2.05; Stoe & Cie GmbH: Darmstadt, Germany, 2004.

S4. Sheldrick, G. M. *SHELX97: Program for Crystal Structure Solution and Refinement*, University of Göttingen, Göttingen, Germany, 1997.

S5. *X-STEP32: Crystallographic Package*, Version 1.07b; Stoe & Cie GmbH: Darmstadt, Germany, 2000.



- S6. L. J. Farrugia, *J. Appl. Crystallogr.*, 1997, **30**, 565.
- S7. Mercury 3.6 Supplied with Cambridge Structural Database; CCDC: Cambridge, U.K., 2015.
- S8. F. Neese, U. Becker, D. Ganyushin, D. G. Liakos, S. Kossmann, T. Petrenko, C. Riplinger, F. Wennmohs, ORCA, 2.7.0; University of Bonn: Bonn, 2009.
- S9. S. H. Vosko, L. Wilk, M. Nusair, *Can. J. Phys.*, 1980, **58**, 1200.
- S10. (a) L. Versluis, T. Ziegler, *J. Chem. Phys.*, 1988, **88**, 322; (b) L. Fan, T. Ziegler, *J. Chem. Phys.*, 1991, **95**, 7401.
- S11. J. P. Perdew, J. A. Chevary, S. H. Vosko, K. A. Jackson, M. R. Pederson, D. J. Singh, C. Fiolhais, *Phys. Rev.*, 1992, **46**, 6671.
- S12. E. van Lenthe, E. J. Baerends, J. G. Snijders, *J. Chem. Phys.*, 1993, **99**, 4597; (b) E. van Lenthe, E. J. Baerends, J. G. Snijders, *J. Chem. Phys.*, 1994, **101**, 9783; (c) E. van Lenthe, R. van Leeuwen, E. J. Baerends, J. G. Snijders, *Int. J. Quantum Chem.*, 1996, **57**, 281.